Journal of Applied Polymer Science

Effect of MWNTs concentration and cooling rate on the morphological, structural, and electrical properties of non-isothermally crystallized PEN/MWNT nanocomposites

Adriana B. Espinoza-Martínez,[1] Carlos A. Ávila-Orta,[2] Víctor J. Cruz-Delgado,[2] Francisco J. Medellín-Rodríguez,[3] Darío Bueno-Baqués,[2] José M. Mata-Padilla[2]

[1]Departamento de Procesos de Transformación de Plásticos, Centro de Investigación en Química Aplicada Boulevard, Enrique Reyna 140 25294 Saltillo, COAH México

[2]Departamento de Materiales Avanzados, Centro de Investigación en Química Aplicada Boulevard, Enrique Reyna 140 25294 Saltillo, COAH México

[3]Departamento de Polimeros, CIEP/FCQ, Universidad Autónoma de San Luis Potosí, Avenida Manuel Nava 6 78210 San Luis Potosí, SLP México

Correspondence to: C. A. Ávila-Orta (E-mail: carlos.avila@ciqa.edu.mx)

ABSTRACT: The effect of multiwall carbon nanotubes (MWNT) concentration and cooling rate on the morphological, structural and electrical properties of non-isothermally crystallized Poly(ethylene naphthalate) nanocomposites (PEN/MWNT) was studied. PEN/MWNT nanocomposites containing 1 and 2 wt % of nanotubes were prepared by melt blending in a mini twin screw extruder. Nanocomposite samples with different degree of crystallinity (X_c) were obtained via non-isothermally crystallization at cooling rates of 2, 10, 20, and 300°C min^{-1}. In this study it was demonstrated that carbon nanotubes and cooling rate strongly influence morphological and structural characteristics of PEN. Calorimetric results showed that the peak crystallization temperature (T_c) of PEN nanocomposites was increased ~9° through heterogeneous nucleation with respect to pure PEN. X-ray diffraction revealed that carbon nanotubes modify the crystalline structure of PEN favoring the formation of β-crystals, and this effect increases with the nanotubes content. On the basis of X-ray scattering analysis, the variation of lamellar thickness revealed that nanotubes promote the formation of lamellar crystals with average thickness of 20 nm at different cooling rates. These structural and morphological changes play an important role on the electrical properties of nanocomposites. It was found that higher concentration of nanotubes and crystallinity promotes electrical conductivity of nanocomposites in the order of semiconductors (until 1×10^{-4} S cm^{-1}) as well as permittivity of 20 at different tested frequencies. This may due to the interconnected networks of nanotubes throughout the crystalline structure formed in PEN nanocomposites. © 2014 Wiley Periodicals, Inc. J. Appl. Polym. Sci. **2015**, *132*, 41765.

KEYWORDS: crystallization; graphene and fullerenes; nanostructured polymers; nanotubes; polyesters

Received 24 June 2014; accepted 11 November 2014
DOI: 10.1002/app.41765

INTRODUCTION

Polymer composites have been widely used in high performance applications for automotive and aerospace industry due to the superior properties resulting from the combination of polymers with fillers, such as elastic modulus, tensile strength, flame resistance, electrical and thermal conductivity, etc.[1–4] The recent introduction of nanofillers has attracted a great deal of interest because of remarkable improvements in the mechanical, flame resistance, and electrical properties at lower filler loadings. Among various nanofillers, carbon nanotubes (CNTs) are now regarded as promising reinforcement in polymer composites due to its unusual properties and high aspect ratio.[5,6] The combination of nanotubes with conventional semi crystalline thermoplastic polymers may provide attractive possibilities to improve the mechanical and electrical properties of these polymers.[7–11] However, as have been reported by other authors[12–15] these properties may depend on the processing conditions and the end morphology which results from the crystallization process. For practical purposes non-isothermally crystallization, is often used as for cooling in industry to create plastic parts.

Therefore, the crystallization behavior for the development of carbon nanotubes-reinforced polymer nanocomposites should

This article was published online on 15 Dec 2014. An error was subsequently identified. This notice is included in the online and print versions to indicate that both have been corrected 29 Dec 2014.

be analyzed to realize the full potential of nanotubes for high performance application.

Poly(ethylene naphthalate) (PEN) is an aromatic polyester that has been used in industry for a wide range of applications, including food packaging materials, fibers, magnetic recording tapes, and flexible printed circuits.[16–19] In general terms, PEN exhibits enhanced mechanical, thermal, gas barrier and chemical resistance properties compared to poly(ethylene terephthalate) PET and poly(butylene terephthalate) (PBT).[20] It has been reported that nanotubes promote the crystallization and the mechanical reinforcement of PEN, as well as the improvement of thermal and electrical properties at low nanotube content.[21–25] The enhancement of these properties not only for PEN but also for a wide variety of semi crystalline polymers gives a guideline for the development of high performance nanotubes based nanocomposites.

Herein, the effect of nanotube concentration and cooling rate on the morphological, structural and electrical properties of non-isothermally crystallized PEN-multiwall carbon nanotubes nanocomposites is studied. It has been reported that carbon nanotubes are good nucleating agents for PEN throughout self-assembly nucleation[23] which make it easier to control the morphology and electrical properties of nanocomposites for their possible application in charge dissipative materials for sensitive items.

EXPERIMENTAL

Materials

Poly(ethylene naphthalate) homopolymer TEONEX® TN8085S with $M_w = 28{,}737$ g gmol^{-1} from Teijin Chemicals was used. Multiwall carbon nanotubes from Nanostructured and Amorphous Materials were used as supplied. The approximate diameter of nanotubes was in the range of 30–50 nm with an aspect ratio of 300–400 and >95% of purity.

Nanocomposites Preparation

PEN and nanotubes were dried in a vacuum oven at 80°C overnight before preparing the nanocomposites. PEN was mixed with two different MWNT weight contents 1 and 2 wt %. The nanocomposites were obtained in a laboratory mini-extruder model LME-120 (Polymer Test) at 300°C. To reach a better dispersion of nanotubes, samples were passed three times through the extruder at 300°C and 30 rpm.

After melt compounding, disc shape samples were molded in a stainless steel mold with dimensions of 8 mm in diameter and 1.5-mm thick. The molded samples were first placed in a hot stage (Mettler, model FP 82 HT) at 300°C for 3 min, to eliminate any previous thermo-mechanical history. After that, the samples were cooled down at different cooling rates: 2, 10, 20, and 300°C min^{-1}. These samples were used for further characterization through X-rays, microscopy, resistivity and capacitance analysis.

Characterization

Crystallization behavior of PEN/MWNT nanocomposites was studied in a Perkin Elmer differential scanning calorimeter (DSC) over the temperature range of 30–300°C under a nitrogen atmosphere. Samples were heated to 300°C at 10°C min^{-1} and held there for 3 min to erase any previous thermal history and then cooled down to 30°C at different cooling rates: 2, 10, 20, and 300°C min^{-1}.

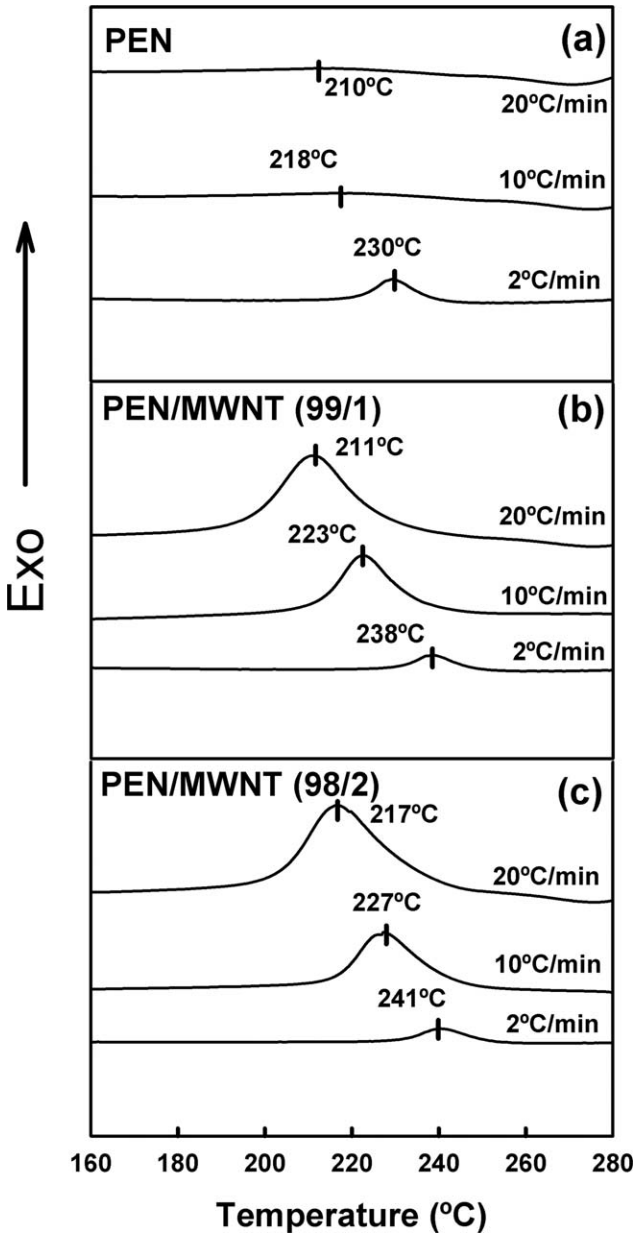

Figure 1. Non-isothermal crystallization curves of (a) pure PEN, (b) PEN/MENT (99/1) and (c) PEN/MWNT (98/2) at different various cooling rates 2, 10, and 20°C min^{-1}.

Simultaneous wide angle X-ray diffraction (WAXD) and small angle X-ray scattering measurements (SAXS) of pure polymer and nanocomposites were measured at room temperature using X-ray scattering equipment SAXSess mc^2 from Anton Paar.

To determine the dispersion of carbon nanotubes in the polymer matrix, nanocomposites were analyzed in a field emission scanning electron microscope (FE-SEM), JEOL model JSM7401F with a voltage of 15 kV. Samples of nanocomposites were cryogenically fractured and coated with Au-Pd.

The volume electrical resistivity was measured by using a digital amplifier, a high voltage amplifier and a charge variable gain amplifier. Each measurement was taken in quadruplicate and the average is reported as result. The resistivity test was

Table I. DSC Results for PEN and PEN/MWNT Nanocomposites Samples Obtained from Cooling Traces at Different Cooling Rates

Sample	Cooling rate (°C min^{-1})	T_c (°C)	ΔH_c (J g^{-1})
PEN	20	210	n.c.
	10	218	n.c.
	2	230	6.3
PEN/MWNT (99/1)	20	211	27.5
	10	223	34.5
	2	238	50.1
PEN/MWNT (98/2)	20	217	33.8
	10	227	47.1
	2	241	60.2

n.c.: Not calculated.

measured in two points following the Cabot EO43 procedure based on ASTM D4496.[26]

Dielectric properties were measured with a capacitance analyzer at ambient temperature at frequencies of 0.1, 1, 10, and 100 kHz. Again, each measurement was taken in quadruplicate and the average is reported as result. The capacitance was determined by the parallel plate method according to ASTM D150 normativity.[27]

RESULTS AND DISCUSSION

Thermal Behavior

Figure 1 shows DSC cooling scans of pure PEN and PEN/MWNT nanocomposites at 2, 10, and 20°C min^{-1}, as a function of MWNT content and the results are summarized in Table I.

At any cooling rate, the crystallization temperature (T_c) increases as the carbon nanotubes content increases from 0 to 2 wt %, which is clearly due to the excellent nucleating effect of the CNT, which enhance the crystallization through heterogeneous nucleation, as reported by other authors.[22,24,25] However, the slower the cooling rate, the more marked the nucleating effect, and the higher the crystallization enthalpy, which is assumed to be due to the larger time the sample is let to remain within the range of crystallization temperatures.[28,29]

At the higher cooling rate of 20°C min^{-1}, the addition of 1 wt % of CNT has a negligible effect on T_c, nonetheless, has a marked effect on the enthalpy of crystallization, which means that, even at these conditions, the CNT do still present a marked nucleating effect on PEN. This nucleating effect may be attributed to the favorable $\pi-\pi$ interactions between PEN and the CNT surface that make it possible.[23]

Morphology

Crystalline Structure. To determine the effect of MWNT on the crystalline structure of PEN WAXD analyses were performed. The samples for pure PEN and PEN/MWNT nanocomposites were that cooled at 2, 10, 20, and 300°C min^{-1}. Figure 2 shows WAXD patterns of PEN and nanocomposites, and their relative crystallinity calculations (X_c) are shown in Table II. X_c was calculated by the method established by Murthy and Minor.[30]

Depending on crystallization conditions PEN generally crystallize in three different crystalline forms α, β, and γ.[31–33] In α-crystals, the structure has extended chains with one chain per unit cell and the crystallographic data, according to Mencik,[31] are: triclinic $a = 6.51$ Å, $b = 5.75$ Å, $c = 13.2$ Å, $\alpha = 81.33°$, $\beta = 144°$, $\gamma = 100°$, and density $\rho = 1.407$ g cm^{-3}. Meanwhile, β-crystals have sinusoidal chains with four chains per unit cell and the crystallographic data are: triclinic $a = 9.26$ Å, $b = 15.59$ Å, $c = 12.73$ Å, $\alpha = 121.6°$, $\beta = 95.57°$, $\gamma = 122.52°$.[32–34] The crystallographic parameters for β-crystals with monoclinic unit cell were proposed by Liu *et al.*[33] where $a = 13.04$ Å, $b = 9.26$ Å, $c = 13$ Å, $\alpha = 131.47°$, $\beta = \gamma = 90°$. In the same report the γ-form was found but their crystallographic parameters were not reported. As observed in Figure 2, when pure PEN is cooled down at 2°C min^{-1} the signals characteristic of α-form appeared, this is, extended chain crystals predominated. When cooling rate increased the samples of pure PEN were amorphous [Figure 2(a)]. With the incorporation of MWNT even for

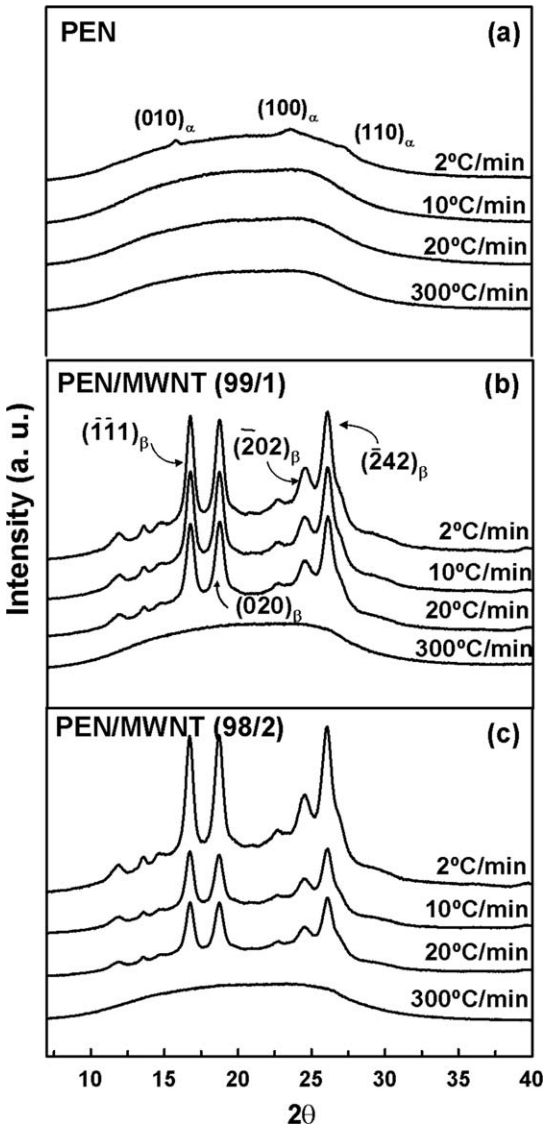

Figure 2. WAXD patterns of pure PEN and nanocomposites crystallized at different cooling rates.

Table II. Relative Crystallinity (X_c) Calculated from WAXD Patterns of Pure PEN and PEN/MWNT Nanocomposites Crystallized at Different Cooling Rates

Sample	Cooling rate (°C min^{-1})	X_c* (%)
PEN	300	n.c.
	20	n.c.
	10	n.c.
	2	4.7
PEN/MWNT (99/1)	300	n.c.
	20	34.7
	10	35.2
	2	38.1
PEN/MWNT (98/2)	300	n.c.
	20	34.9
	10	36.1
	2	38.6

n.c. Not calculated.

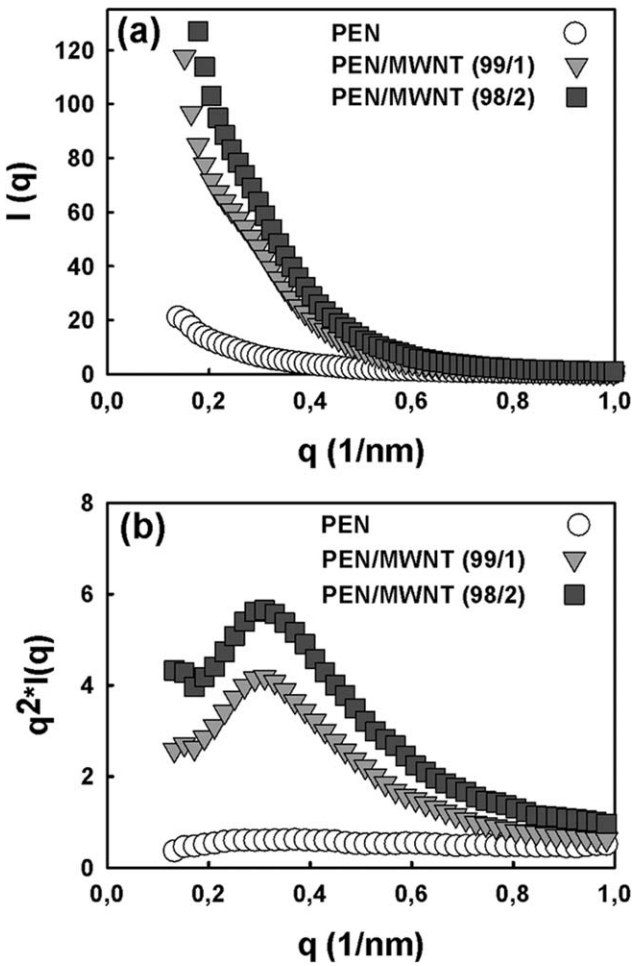

Figure 3. SAXS patterns of pure PEN and nanocomposites (a) experimental data and (b) Lorentz corrected plots.

Table III. Maximum Scattering Vector (q_{max}) and Long Period or Periodicity (L) of Pure PEN and PEN/MWNT Nanocomposites

Sample	Cooling rate (°C min^{-1})	q_{max} (1/nm)	L (nm)
PEN	20	n.c.	n.c.
	10	n.c.	n.c.
	2	0.39	16.12
PEN/MWNT (99/1)	20	0.31	20.24
	10	0.31	20.24
	2	0.30	20.68
PEN/MWNT (98/2)	20	0.31	20.24
	10	0.30	20.68
	2	0.29	21.62

n.c. Not calculated.

samples cooled at the higher cooling rates additional peaks appeared. The planes identified were 111, 020, 202, 242, and occur when β-crystals are formed.[30] Kim *et al.*,[35] found similar reflections in PEN/MWNT nanocomposites, where the influence of MWNT on crystalline structure and mechanical properties of PEN nanocomposites was studied. In our case, as the cooling rate decreased the intensity of patterns in nanocomposites became stronger indicating that large β crystals were developed. These important changes associated with crystalline structure and crystallinity may be attributed to the easily adsorption of PEN chains on nanotubes by means of aromatic self-assembly nucleation, as previously reported.[23]

Lamellar Structure. The structure of semicrystalline polymers consists of lamellar crystals periodically ordered enclosed by amorphous phases. Periodicity, known as long period (L), can be calculated by substituting the value of the maximum peak position of dispersion vector (q_{max}) in the eq. (1). q_{max} is obtained from dispersion plot with the Lorentz correction.[36]

$$L = \frac{2\pi}{q_{max}} \quad (1)$$

With the objective to analyze the influence of carbon nanotubes in the periodicity of PEN SAXS studies were performed. Figure 3 shows experimental and Lorentz corrected SAXS patterns of nanocomposites PEN/MWNT and pure PEN cooled at 10°C min^{-1}. It is observed in [Figure 3(a)] that no peaks appeared in pure PEN patterns. However, for PEN/MWNT nanocomposites the intensity of experimental patterns [Figure 3(a)] increased. When observing Lorentz corrected plots [Figure 3(b)] it is noticed that pure PEN shows no scattering peaks which can be due to the presence of large amorphous areas between crystalline lamellas. PEN nanocomposites showed well defined peaks that may be attributed to the nucleating activity of nanotubes promoting the formation of large crystals. Periodicity values of pure PEN and nanocomposites cooled at 2, 10, and 20°C min^{-1} are shown in Table III. For pure PEN it was not possible to calculate periodicity when samples were cooled at 20 and 10°C min^{-1} due to the lack of scattering signals but PEN cooled at 2°C min^{-1} had a periodicity of 16.2 nm. When nanotubes were added to PEN, thickness of lamellar crystals

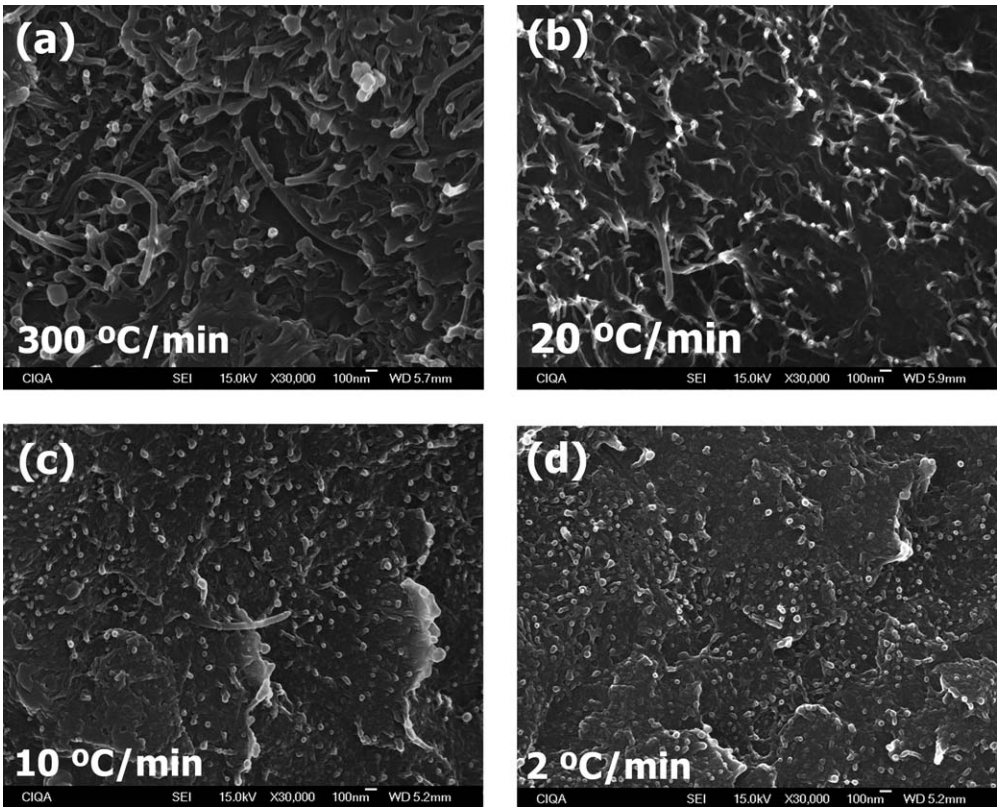

Figure 4. FE-SEM images of the fractured surface of PEN/MWNT (98/2) nanocomposites crystallized at cooling rates of: (a), 300°C min^{-1}, (b) 20°C min^{-1}, (c) 10°C min^{-1}, and 2°C min^{-1} (d).

increased up to 5 nm at the higher loading. This observation shows that carbon nanotubes are effective nucleating agents and promotes lamellar thickening for the growth of large crystals, at the concentration of nanotubes studied. This may explain the change from α to β crystals of PEN after incorporating 1 and 2 wt % of carbon nanotubes. Logakis *et al.*[37] reported for Nylon-6 nanocomposites that at MWNT contents higher than 2 wt % the formation of large and perfect crystallites are prevented due to limited space and restrictions imposed to the motion of the polymer chains.

Dispersion of Carbon Nanotubes. To study the dispersion of nanotubes in PEN the cryogenic fractured surfaces of nanocomposites were observed by FE-SEM. In Figure 4 FE-SEM images of nanocomposites PEN/MWNT (98/2) cooled at different cooling rates are shown. In all the cases a homogeneous dispersion of nanotubes throughout PEN was observed.

It can be thought that all PEN/CNT samples containing 2 wt % CNT had a similar distribution/dispersion degree, since they all were prepared in the same way. Nonetheless, Figure 4 shows that after heating up to 300°C and submitting these to four different cooling rates, produces strikingly different apparent morphologies. In this case, as the cooling rate slows down, PEN molecules have more time to diffuse through nanotubes entanglements. This phenomenon could explain the electrical properties of nanocomposites.

Electrical Behavior

Electrical Conductivity. The volume electrical conductivity of nanocomposites crystallized at different cooling rates and contents of nanotubes is shown in Figure 5. It can be observed that conductivity increased with the addition of CNT up to 1×10^{-7} S cm^{-1} (1 wt %) and 1×10^{-4} S cm^{-1} (2 wt %). Analyzing the electrical conductivity of PEN/MWNT (98/2) nanocomposites showed a slight decrease in conductivity as increased cooling rate. This may be due to the less ordered structure of PEN molecules in amorphous samples which prevent the free trajectory for electron transfer. It may be suggested that the electrical conductivity mechanism in nanocomposites is given as a function of cooling rate (crystallinity) and nanotubes content. At higher nanotubes content the formation of interconnected networks

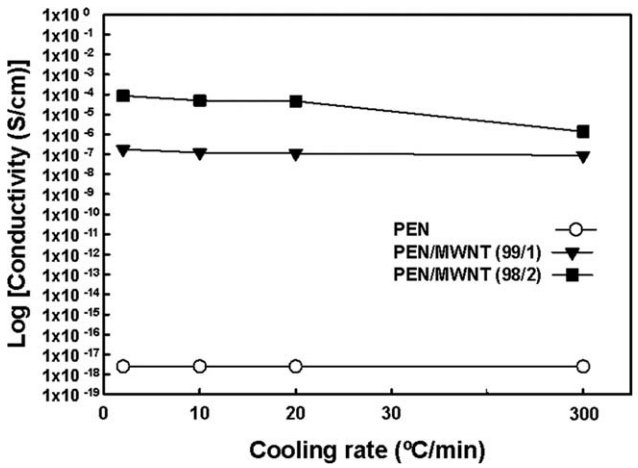

Figure 5. Electrical conductivity of PEN/MWNT nanocomposites crystallized at different cooling rates.

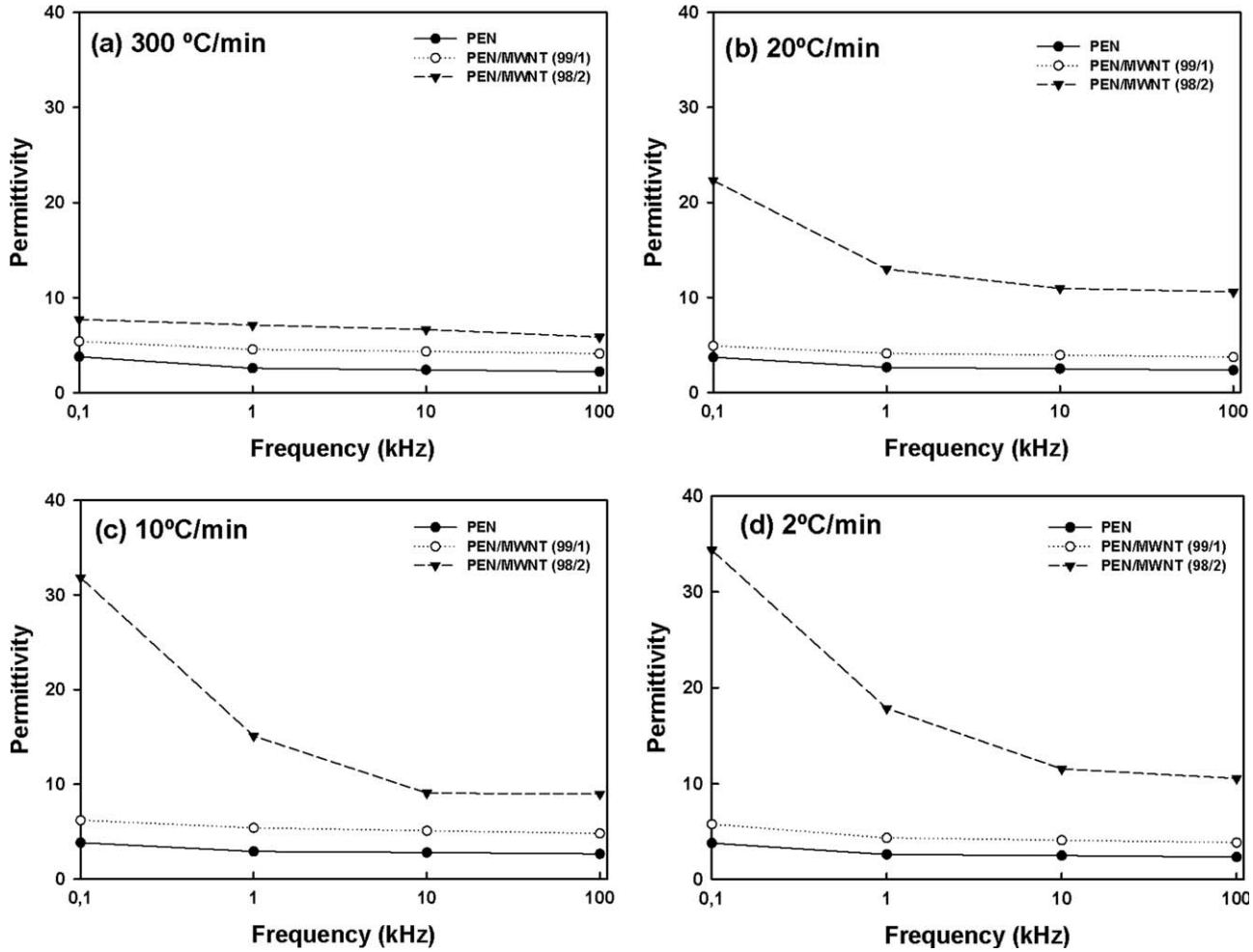

Figure 6. Permittivity of PEN and PEN/MWNT nanocomposites crystallized at different cooling rates.

throughout the polymer matrix is promoted at low cooling rates and electrical conductivity is improved. Based on the achieved conductivities, these materials can be considered as semiconductors[38] and are proposed for the manufacture of charge dissipation materials for sensitive items according to the normativity of Electrostatic Discharge Association (ESD) and the American National Standards Institute in the ANSI/ESD S541–2008.[39] Our materials have new competitive advantages with respect to those reported by different authors for polymer-CNT systems with similar conductivities.[40–46] First, they were prepared by means of a simple melt compounding methodology that prevents the use of intermediate compounding steps or dangerous solvents. Second, the structural and integrity damage of CNT is prevented due to they were not functionalized by covalent methods. In this case, it was took advantage of the chemical structure of PEN and its ability to easily crystallize by means of aromatic self-assembly nucleation[23] which makes the methodology a simple way for the fabrication of electrostatic dissipation materials with controlled morphology.

Permittivity. It is well known that polymers are generally good insulating materials due to their physical and chemical properties.[43] But, the inclusion of conductive fillers can modify the dielectric properties of polymer composites. Permittivity or dielectric constants at different frequencies of PEN and PEN/MWNT nanocomposites crystallized at different cooling rates are shown in Figure 6. It is observed that the permittivity of PEN increases with the content of MWNTs. The permittivity of the pure PEN at different frequencies is found around 3, and in nanocomposites with 1 and 2 wt % of nanotubes reaches an average of 5 and 17 respectively, which is approximately two and five times of the pure PEN. As observed in Figure 6 there are important changes in dielectric behavior of nanocomposites with 2 wt % when decreasing the cooling rate. For example, it is observed that permittivity evaluated at 0.1 kHz of nanocomposites cooled at 2 and 10°C min^{-1} is 30 for both cases, and 7 for the higher cooling rate (300°C min^{-1}). These changes in the dielectric constant can be also explained in terms of the structure of the nanocomposites where the ordered structures imply a better distribution of the charges and higher dielectric constant. At the same time there may be ordered percolation paths as showed in the electrical conductivity results. Some authors have reported that the increase in permittivity of conductive-dielectric (conductive filler-dielectric polymer) nanocomposites is directly associated to the percolation phenomena.[44,47] However, to ensure if PEN nanocomposites serves as dual materials it is necessary to perform a more complete analysis of their

charge and discharge cycle as part of the next step of this research.

CONCLUSIONS

PEN/MWNT nanocomposites were prepared by melt compounding with contents of nanotubes of 1 and 2 wt % of MWNT, and the effects of nanotubes concentration and cooling rate on morphology, structure and electrical properties were studied. The peak crystallization temperature, the crystalline content and the lamellar thickness of PEN were significantly improved with the introduction of nanotubes and decreasing the cooling rate, and these enhancing effects were more pronounced in nanocomposites with 2 wt % of CNT. The incorporation of more MWNTs facilitates to the formation of β-crystals in the PEN/MWNT nanocomposites. The dispersed CNTs played an important role in improving the morphology of PEN/MWNT nanocomposites by acting as effective nucleating agents due to the favorable interactions between the surface of the nanotubes and the naphthalene group of PEN chains. The improvement in the electrical conductivity and permittivity of PEN/MWNT nanocomposites was attributed to a combined effect of crystalline morphology and nanotubes content. We believe that our methodology developed for the preparation of semiconductor nanocomposites has competitive advantages for the fabrication of electrostatic dissipation materials with controlled morphology.

ACKNOWLEDGMENTS

The authors thank the CONACyT for the financial support in the projects J49551, 232753 and the CIQA project 6162. They thank Janett Valdez, Gilberto Hurtado, Blanca Huerta, Guadalupe Méndez, Myriam Lozano, Jesús Cepeda, Jesús Rodríguez, and Adán Herrera for the technical support. We also wish to thank the Mexican National Laboratory of Graphene (Laboratorio Nacional de Materiales Grafénicos) for their financial support through CONACYT's grant, number 232753.

REFERENCES

1. Kim, H.-J.; Nam, S.-M.; Koh, J.-H. *J. Nanosci. Nanotechnol.* **2014**, *14*, 7915.
2. Molefi, J. A.; Luyt, A. S.; Krupa, I. *J. Mater. Sci.* **2009**, *45*, 82.
3. Elleithy, R. H.; Ali, I.; Ali, M. A.; Al-Zahrani, S. M. *J. Appl. Polym. Sci.* **2010**, *117*, 2413.
4. Liu, L.; Hu, J.; Zhuo, J.; Jiao, C.; Chen, X.; Li, S. *Polym. Degrad. Stab.* **2014**, *104*, 87.
5. Yakobson, B. I.; Avouris, P. *Top. Phys.* **2001**, *80*, 287.
6. Coleman, J. N.; Khan, U.; Blau, W. J.; Gun'ko, Y. K. *Carbon N. Y.* **2006**, *44*, 1624.
7. Dong, Q.; Li, Y.; Han, C.; Zhang, X.; Xu, K.; Zhang, H.; Dong, L. *J. Appl. Polym. Sci.* **2013**, *130*, 3919.
8. Seo, G.-B.; Kim, G.-H. *J. Appl. Polym. Sci.* **2014**, *131*, DOI: 10.1002/app.40129.
9. Puch, F.; Hopmann, C. *J. Appl. Polym. Sci.* **2014**, *131*.
10. Vasileiou, A. A.; Docoslis, A.; Kontopoulou, M.; Xiang, P.; Ye, Z. *Polymer* **2013**, *54*, 5230.
11. Mai, F.; Pan, D.; Gao, X.; Yao, M.; Deng, H.; Wang, K.; Chen, F.; Fu, Q. *Polym. Int.* **2011**, *60*, 1646.
12. Tambe, P. B.; Bhattacharyya, A. R.; Kulkarni, A. R. *J. Appl. Polym. Sci.* **2013**, *127*, 1017.
13. Ávila-Orta, C. A.; Raudry-López, C. E.; Dávila-Rodríguez, M. V.; Aguirre-Figueroa, Y. A.; Cruz-Delgado, V. J.; Neira-Velázquez, M. G.; Medellín-Rodríguez, F. J.; Hsiao, B. S. *Int. J. Polym. Mater.* **2013**, *62*, 635.
14. Miquelard-Garnier, G.; Guinault, A.; Fromonteil, D.; Delalande, S.; Sollogoub, C. *Polymer* **2013**, *54*, 4290.
15. Cruz-Delgado, V. J.; Ávila-Orta, C. A.; Espinoza-Martínez, A. B.; Mata-Padilla, J. M.; Solis-Rosales, S. G.; Jalbout, A. F.; Medellín-Rodríguez, F. J.; Hsiao, B. S. *Polymer* **2014**, *55*, 642.
16. Zhang, H.; Ward, I. M. *Macromolecules* **1995**, *28*, 7622.
17. Weick, B. L.; Bhushan, B. *Wear* **1995**, *190*, 28.
18. Dennler, G.; Lungenschmied, C.; Neugebauer, H.; Sariciftci, N. S.; Latrèche, M.; Czeremuszkin, G.; Wertheimer, M. R. *Thin Solid Films* **2006**, *511/512*, 349.
19. Utsumi, S. Uniaxially High-ordered Polyethylene Naphthalate Film for Liquid Crystal Panel Substrates, iafoil Company, Limited, Tokyo Japan. U.S. Pat. 4,799,772 (**1989**).
20. Ito, M.; Kikutani, T. In: Handbook of Thermoplastic Polyesters, Homopolymers, Copolymers, Blends and Composites; Fakirov, S., Ed.; Wiley-VCH: Weinheim, **2002**; p 463.
21. Kim, J. Y.; Han, S. I.; Kim, D. K.; Kim, S. H. *Compos. A Appl. Sci. Manuf.* **2009**, *40*, 45.
22. Kim, J. Y.; Han, S. I.; Hong, S. *Polymer* **2008**, *49*, 3335.
23. Espinoza-Martínez, A.; Avila-Orta, C.; Cruz-Delgado, V.; Olvera-Neria, O.; González-Torres, J.; Medellín-Rodríguez, F. J. *J. Nanomater.* **2012**, 2012, 1.
24. Wu, D.; Wu, L.; Yu, G.; Xu, B.; Zhang, M. *Polym. Eng. Sci.* **2008**, *48*, 1057.
25. Kim, J. Y.; Park, H. S.; Kim, S. H. *J. Appl. Polym. Sci.* **2006**, *103*, 1450.
26. ASTM D4496—04e1 Standard Test Method for D C Resistance or Conductance of Moderately Conductive Materials. Available at: http://www.astm.org/Standards/D4496.htm (accessed Oct 5, 2012).
27. ASTM D150—11 Standard Test Methods for AC Loss Characteristics and Permittivity (Dielectric Constant) of Solid Electrical Insulation. Available at: http://www.astm.org/Standards/D150.htm (accessed Oct 5, **2012**.
28. Xu, W.; Ge, M.; He, P. *J. Polym. Sci. B Polym. Phys.* **2002**, *40*, 408.
29. Kim, S. H.; Ahn, S. H.; Hirai, T. *Polymer* **2003**, *44*, 5625.
30. Murthy, N. S.; Minor, H. *Polymer* **1990**, *31*, 996.
31. Mencik, Z. *J. Polym. Sci. Polym. Phys. Ed.* **1975**, *13*, 2173.
32. Zachmann, H. G. *Die Makromol. Chem.* **1985**, *12*, 175.
33. Liu, J.; Sidoti, G.; Hommema, J. A.; Geil, P. H.; Kim, J. C.; Cakmak, M. *J. Macromol. Sci. B* **1998**, *37*, 567.

34. Buchner, S.; Wiswe, D.; Zachmann, H. *Polymer* **1989**, *30*, 480.

35. Kim, J. Y.; Han, S.-I.; Kim, S. H. *Polym. Eng. Sci.* **2007**, *47*, 1715.

36. Cser, F. *J. Appl. Polym. Sci.* **2001**, *80*, 2300.

37. Logakis, E.; Pandis, C.; Peoglos, V.; Pissis, P.; Stergiou, C.; Pionteck, J.; Pötschke, P.; Micušík, M.; Omastová, M. *J. Polym. Sci. B Polym. Phys.* **2009**, *47*, 764.

38. Saini, P.; Choudhary, V.; Dhawan, S. K. *Polym. Adv. Technol.* **2012**, *23*, 343.

39. Brent Beame. ANSI/ESD S541–2008; Rome:, **2008**.

40. Nayak, L.; Chaki, T. K.; Khastgir, D. *J. Appl. Polym. Sci.* **2014**, *131*.

41. Dubnikova, I.; Kuvardina, E.; Krasheninnikov, V.; Lomakin, S.; Tchmutin, I.; Kuznetsov, S. *J. Appl. Polym. Sci.* **2010**, *117*, 259.

42. Zhu, X.-D.; Zang, C.-G.; Jiao, Q.-J. *J. Appl. Polym. Sci.* **2014**, 131.

43. Ghosh, P. Polymer Science and Technology: Plastics, Rubbers, Blends, and Composites; Tata McGraw-Hill Education: New Delhi, India, **2001**; p 497.

44. Hanemann, T.; Szabó, D. V. *Materials (Basel)* **2010**, *3*, 3468.

45. Saini, P.; Choudhary, V. J. *Nanopart. Res.* **2013**, *15*, 1415.

46. Chubb, J. N. *J. Electrostat.* **2007**, *65*, 607.

47. Dang, Z. M.; Wu, J. P.; Xu, H. P.; Yao, S. H.; Jiang, M. J.; Bai, J. *Appl. Phys. Lett.* **2007**, *91*, 072912.